Acta Geodyn. Geomater., Vol. 23, No. 2 (222), 279–288, 2026
DOI: 10.13168/AGG.2026.0018
journal homepage: https://www.irsm.cas.cz/acta

C
ORIGINAL PAPER

INTEGRATED BENEFICIATION STUDIES ON LOW-GRADE MANGANESE ORES FROM MOHMAND, PAKISTAN: INSIGHTS FROM PETROGRAPHY, GEOCHEMISTRY AND XRD ANALYSIS

Muhammad SHAHAB [1] *, Irfan ULLAH [2)], Liaqat ALI [2)] *, Ishaq AHMAD [3)], Saira SHERIN [3)], Fahad ALSHEHRI [4)], George KONTAKIOTIS [5)], Raham JALIL [6)] and Syed Mamoon SIYAR [7)]

[1)] *Abdullah Alrushaid Chair for Earth Science Remote Sensing Research, Geology and Geophysics Department, King Saud University, Riyadh 11451, Saudi Arabia*
[2)] *National Centre of Excellence in Geology, University of Peshawar, Peshawar 25130, Pakistan*
[3)] *Department of Mining Engineering, University of Engineering and Technology Peshawar*
[4)] *Department of Geology and Geophysics, College of Science, King Saud University, P.O. Box 2455, Riyadh, 11451, Saudi Arabia*
[5)] *Department of Historical Geology-Paleontology, Faculty of Geology and Geo-environment, School of Earth Sciences, National and Kapodistrian University of Athens, Panepistimiopolis, Zografou, 15784 Athens, Greece*
[6)] *School of Natural Sciences, Macquarie University, North Ryde 2109, Australia*
[7)] *Department of Geology, University of Malakand, Chakdara 18800, Pakistan*

**Corresponding author's e-mail:* mshahab.c@ksu.edu.sa; liaqat.nceg@uop.edu.pk

ARTICLE INFO

Article history:
Received 21 January 2025
Accepted 5 January 2026
Available online 11 June 2026

Keywords:
Mineralogy
Beneficiation
Mohmand
Pakistan

ABSTRACT

Beneficiation investigations targeting the low-grade manganese ores situated within the boundaries of the Mohmand district were executed with the aim of connecting their potential for integration into manganese-centric industrial applications. A meticulous delineation of these ores was undertaken through a comprehensive amalgamation of petrographic, geochemical and mineralogical analyses, followed by experimental assessments to determine paths for their value upgrading. Employing physical beneficiation methodologies, notably gravity and magnetic separation, led to discernible enhancements in the manganese-to-iron (Mn:Fe) ratio, thus substantiating the feasibility of upgrading these ores.

Geochemical characterization classified the ores as siliceous manganese ores, while mineralogical scrutiny delineated braunite and pyrolusite as the principal manganese-bearing minerals. Quartz (SiO_2) emerged as the predominant gangue mineral, accompanied by minor quantities of calcite ($CaCO_3$) and hematite (Fe_2O_3). Noteworthy is the fractured nature of the manganese minerals, compounded by secondary quartz infillings. Beneficiation endeavors underscored the efficiency of coarser grain sizes in achieving optimal liberation degrees for these low-grade ores.

The findings underscore the potential for substantial augmentation in manganese content, evidenced by an elevation from 24 wt. % to 43.6 wt. % through gravity separation, coupled with a recovery rate of 66.49 %. Magnetic separation interventions yielded further improvements, elevating the concentration to 45.96 wt. %, while concurrently enhancing recovery rates to 89.17 %. The cumulative outcomes underscore the viability of integrating these beneficiation strategies into industrial processes, thereby fostering enhanced utilization of low-grade manganese ores within the Mohmand district.

1. INTRODUCTION

Manganese (Mn) is a transition metal with atomic number 25 that plays a critical role in both geological and industrial systems. In nature, manganese rarely occurs in its native form; instead, it is commonly associated with iron and other metallic elements within a wide range of mineral assemblages. Economically significant manganese deposits are dominated by oxide minerals, particularly pyrolusite (MnO_2), along with other oxide and oxyhydroxide phases such as hausmannite (Mn_3O_4) and manganite (MnO(OH)). In addition to these oxides, manganese is also present in carbonate, silicate, and sulfide minerals, including rhodochrosite ($MnCO_3$), rhodonite ($MnSiO_3$), and alabandite (MnS). Among these, pyrolusite represents the most important ore mineral due to its high manganese content, reaching approximately 63.2 wt.% Mn (Zhang and Cheng, 2007; Mehdilo et al., 2013; Din et al., 2025). Mn deposits, including continental sedimentary sequences and ophiolites, form in various tectonic settings and can be divided into three broad categories. Hydrothermally, Mn deposits are epithermal veins and laminated and irregular bodies and are commonly strata-bound. Deposition usually occurs adjacent to either spreading centers or intraplate seamounts or may be related to subduction associated with island arcs (Polgári et al., 2012; Baba et al., 2014; Öksüz and Okuyucu, 2014). Manganese ores can also accumulate in sedimentary deposits or metamorphic rocks, typically forming nodules on the ocean floor (Kogel et al., 2006). Mn is crucial in the steel, glass, and chemical industries. It is mainly used in various industries for alloys (e.g., FeMn and SiMn) and various compounds (e.g., $MnSO_4$, $MnCl_2$, KMn). In the steel industry, oxygen and sulfur are removed, which imparts hardness, malleability, and tenacity to steel. Steel made of ferromanganese and silico-

Cite this article as: Shahab M, Ullah I, Ali L, Ahmad I, Sherin S, Alshehri F, Kontakiotis G, Jalil R, Siyar SM: Integrated beneficiation studies on low-grade manganese ores from Mohmand, Pakistan: Insights from petrography, geochemistry and XRD analysis. Acta Geodyn. Geomater., 23, No. 2 (222), 279–288, 2026. DOI: 10.13168/AGG.2026.0018

manganese is used in construction and transportation machinery (Siddiquie et al., 2015; Rehman et al., 2020; Rao et al., 2026). Chemical grade produces chemicals, batteries, glass, plant food, paints, pigments, and the textile industry. It is also used as a water purifier, catalyst, and oxygen carrier for chemical looping combustion (CLC) (Mehdilo and Irannajad, 2014; Haider et al., 2016). Globally, most of the Mn (90-95 %) produced annually (with a Mn content greater than 40 %) is used in the steel industry as a deoxidizer and desulfurizer. The remaining (5-10 %) is consumed by other industries, such as chemicals, paint, fertilizer, batteries, and glass (Lasheen et al., 2009; Sudharsan et al., 2024).

The former USSR, Brazil, South Africa, Australia, Gabon, and India are the primary sources of manganese. Approximately 85 % of the world's pyrolusite is produced in South Africa and Russia (Zhang and Cheng, 2007; Sunet al., 2025). In Pakistan, Mn deposits are low to medium grade; those associated with continental sedimentary sequences are reported in Chura Gali, Galdanian, and Kakul from the Hazara region of Khyber Pakhtunkhwa Province. Similarly, Mn deposits that are associated with ophiolitic rocks have been reported in North Waziristan, Bajaur and Lasbela-Khuzdar, Zhob (Naseem et al., 1997; Shah and Khan, 1999; Shah and Moon, 2004; Ding et al., 2025).

Globally, manganese deposits are predominantly characterized by low- to medium-grade ores, with average manganese contents typically ranging between ~20 and 35 wt.% Mn. Rapid industrialization and the increasing demand for steel—particularly in developing economies—have significantly intensified the consumption of manganese ores. Concurrently, easily accessible high-grade manganese resources are being progressively depleted, creating supply constraints for manganese-dependent industries. As a result, a substantial proportion of manganese-bearing material with Mn or MnO contents below conventional market thresholds (commonly < 25 wt.%) is classified as low-grade and is often stockpiled or discarded due to economic and technical limitations. However, the sustainable utilization of these low-grade manganese ores has become increasingly important to ensure long-term resource security. To upgrade such materials to marketable grades, a variety of beneficiation techniques are routinely applied worldwide, including gravity separation, magnetic separation, and froth flotation, which have proven effective in improving manganese grade and recovery from low-grade ores (Ahmad, 2016; Peng et al., 2018; Liu et al., 2019; Singh et al., 2020). In Pakistan, due to an unprofessional attitude towards mining, medium-grade ores are separated through smelting, which is directly used by the metallurgical industry for steel production. Moreover, low-grade ores (with MnO contents > 25 %) are dumped at mining sites and are considered uneconomical, creating severe environmental issues. Therefore, this study aimed to upgrade these low-grade ores for use in the steel industry.

2. STUDY AREA

The study area is located in the vicinity of Inzari–Miagan village, District Mohmand, as shown on the Survey of Pakistan Toposheet No. 38 N/06, and is geographically bounded by 34°36′97″ N latitude and 71°20′23″ E longitude. It lies 84 km from Peshawar city; it is easily accessible from Peshawar via the Mohmand-Bajuar Road. Mohmand is bordered by the Bajaur district to the north, the Khyber district to the south, the Malakand and Charsadda districts to the east, and the Peshawar district to the southeast. Geologically, the study area is located in the Nawagi Melange, which is a subzone of the Indus Suture Melange Zone and lies to the north of the main mantle thrust (MMT) and to the south of the Kohistan Fault.

3. MATERIALS AND METHODS

The low-grade manganese ores of the Mohmand district were geochemically categorized as low-grade Mn ores (MnO < 25 %). This categorization was based on preliminary bulk chemical analyses carried out using atomic absorption spectrometry (AAS), which indicated MnO concentrations consistently below the economic cutoff grade for high-grade Mn ores. Eight samples were crushed using a tungsten grinding mill to reduce the size to less than < 200 μm and were stored in plastic bags to avoid contamination. The samples were digested using a mixed-acid digestion procedure involving HCl, HNO_3, HF, and $HClO_4$, selected to ensure complete dissolution of Mn-bearing and associated silicate phases, prior to geochemical analysis via atomic absorption spectrometry (AAS). Two (02) powder samples were studied using X-ray diffraction (XRD) to identify various Mn-bearing minerals and gangue minerals associated with these low-grade ores. Polished thin sections were made from (08) samples for transmitted and reflected light microscopy to examine mineralogy, textures, and ore–gangue relationships. Scanning electron microscopy (SEM) was used to analyse the Mn minerals at high magnifications to identify the rock-forming minerals and their textures, grain sizes, and grain interactions (Shahab et al.,2025; Alshehri et al., 2025).

For continuity, SEM analysis was conducted after petrographic examination and XRD analysis to better correlate mineral textures with mineralogical phases. Similarly, polished chips (03) were prepared for SEM analysis at National Centre of Excellence (NCE) in Geology, University of Peshawar.

The methodology followed for the beneficiation studies is illustrated in Figure 2. Approximately 30 kg of bulk low-grade Mn ore was initially collected from the study area; from this bulk sample, a representative sub-sample of 10 kg was obtained for laboratory-scale beneficiation experiments, as shown in Figure 2. The samples were crushed using a laboratory-scale jaw crusher to reduce the size to > 3 mm; the grain size of the obtained product was further reduced to less than > 1 mm using a laboratory-scale disc crusher at the Department of Mining Engineering, UET Peshawar. Sample splitting was carried out using a mechanical riffle splitter, as illustrated in Figure 2, to ensure

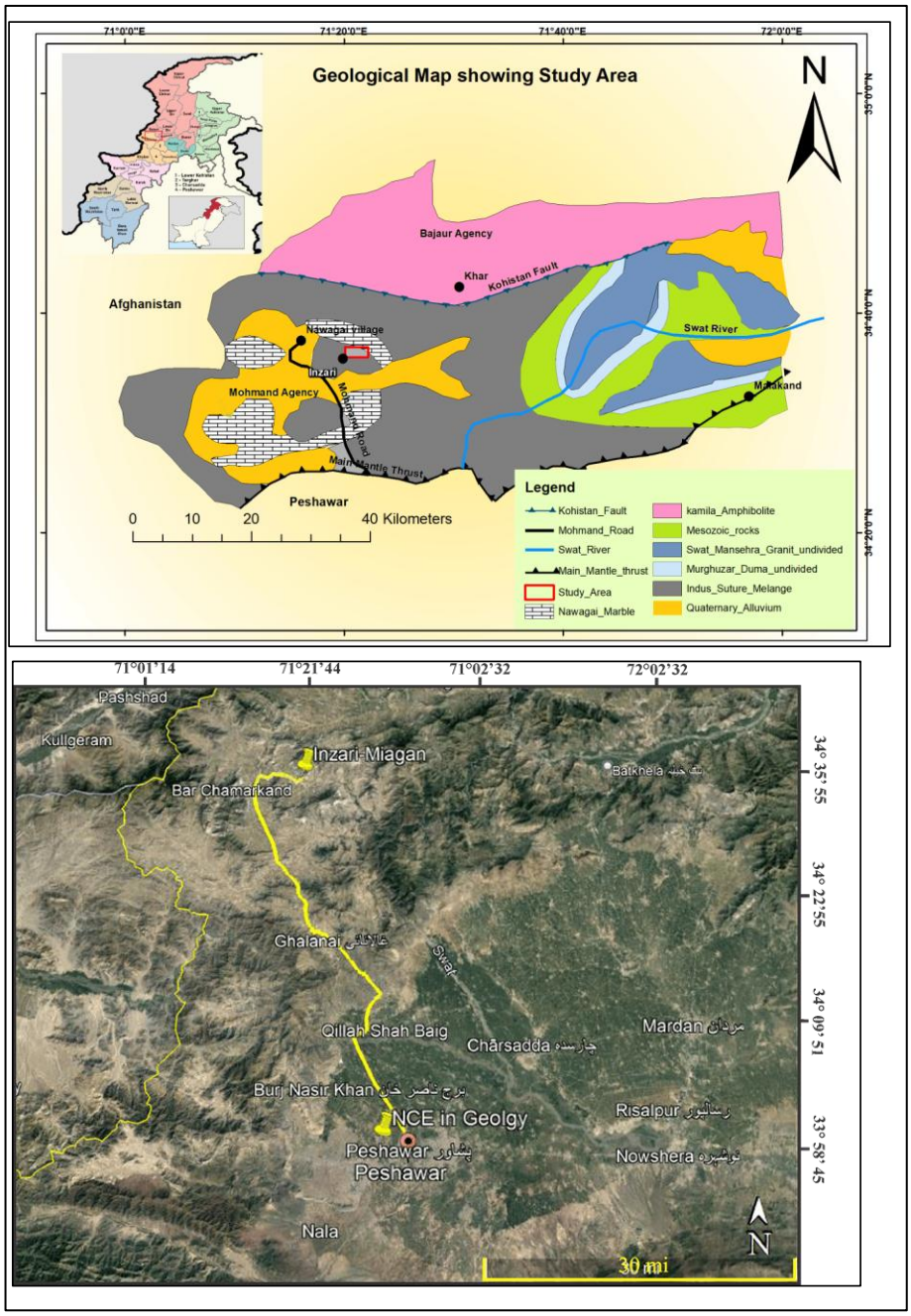

Fig. 1 Figure 1 showing the localized geological map and Location map of the study area.

representative sub-sampling and to minimize sampling bias. Approximately 10 kg of the crushed sample was coned and quartered, and four representative samples of fractions +800 to +400 µm size fractions were taken and stored in plastic bags for beneficiation studies. ASTM standard sieves were used for grain size analysis. Based on detailed mineralogical observations (XRD, petrography, and SEM) and bulk chemical composition, appropriate physical beneficiation techniques were selected. The dominance of Mn oxides with higher specific gravity compared to silicate gangue minerals justified the use of gravity separation techniques (Ullah et al., 2025). Gravity separation experiments were carried out using a laboratory-scale shaking table. The shaking table was operated at variable deck inclination angles ranging from 2° to 5°, as shown in Figure 2, to optimize Mn recovery and concentrate grade.

Magnetic separation was employed to remove iron-bearing minerals associated with the Mn ores. A laboratory-scale magnetic separator was operated at a field intensity of approximately 8,000–12,000 gauss to selectively separate magnetic Fe-bearing phases from the non-magnetic Mn-rich fraction. The beneficiated products were subsequently analyzed geochemically using AAS at the NCE, University of Peshawar. Mn grades and recoveries were calculated to evaluate the efficiency of the applied beneficiation techniques.

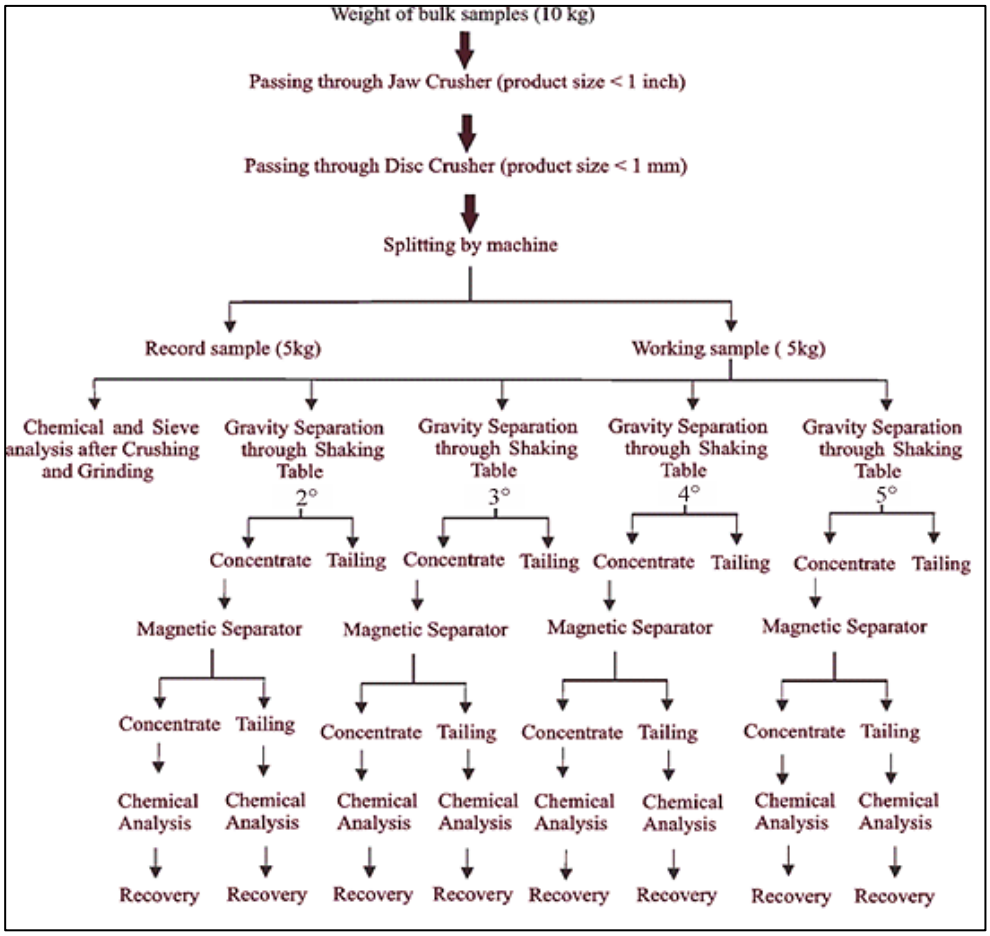

Fig. 2 Workflow of the procedure followed for beneficiation.

4. RESULTS

4.1. CHEMICAL COMPOSITION AND MINERALOGY

Eight representative low-grade Mn ore samples were analyzed using atomic absorption spectrometry (AAS) to determine the concentrations of major oxides, and the results are presented in Table 1. The analyses show that the ores are characterized by a low manganese content, with an average of 24 % MnO, accompanied by high silica (56.35 % SiO_2) and minor iron oxide (2.61 % Fe_2O_3) (Table 1).

X-ray diffraction (XRD) analysis (Fig. 3) reveals that the dominant Mn-bearing mineral phases are pyrolusite (MnO_2) and braunite ($Mn^{2+}Mn^{6+}{}_6[O_8SiO_4]$). The principal gangue mineral is silica (SiO_2), while calcite ($CaCO_3$) and hematite (Fe_2O_3) occur as minor accessory phases.

4.2. MICROSCOPIC OBSERVATIONS

Petrographic observations under transmitted and reflected light microscopy indicate that the dominant gangue mineral in the low-grade Mn ores is secondary silica, occurring mainly as quartz veins that crosscut and intrude the pre-existing Mn ore minerals. The secondary nature of silica is inferred from its vein-like geometry, sharp planar to concave–convex intrusive contacts with Mn minerals, and its crosscutting relationship, which post-dates Mn mineralization (Figs. 4A–4E). These quartz veins display sharp planar contacts with the Mn-bearing phases, as observed in Figures 4B, 4D, and 4E, whereas Figure 4A illustrates fine-grained silica (chert) enclosed within Mn minerals, indicating growth.

Modal estimation from petrographic analysis shows that coarse-grained quartz constitutes more than 65 vol.% of the low-grade Mn ores, consistent with observations in the photomicrographs (Figs. 4B–4E). Fine-grained quartz (chert) occurs as enclosed domains within Mn ore minerals and exhibits sutured to concave–convex grain boundaries, reflecting contemporaneous deposition and post-depositional recrystallization (Fig. 4A). Figure 4C, newly cited here, shows disseminated hematite grains occurring within Mn ore matrices, further supporting the complex paragenetic sequence. Hematite occurs as fine disseminations within Mn minerals, as shown in Figure 4F.

SEM observations further corroborate the petrographic findings. Mn-bearing minerals appear in light-gray contrast under SEM and occur predominantly in massive aggregates with an average grain size exceeding 400 µm. In contrast, silica appears as dark-toned phases that crosscut Mn minerals and display planar to concave–convex contacts, confirming its secondary origin (Figs. 5A and 5D). Pyrolusite grains exhibit elongated spindle-shaped morphologies, whereas braunite occurs as

Table 1 Geochemical analysis results of the significant oxides in (wt %) of the low-grade Mn ores.

Sample	IMS-1	IMS-2	IMS-3	IMS-4	IMS-5	IMS-6	IMS-7	IMS-8	Average
SiO_2	57.21	62.23	55.61	52.45	56.01	55.28	54.02	57.96	56.35
TiO_2	0.34	0.09	0.20	0.05	0.09	0.06	0.46	0.23	0.19
Al_2O_3	2.18	3.06	3.23	2.98	3.23	3.23	2.55	1.99	2.806
Fe_2O_3	2.11	2.35	2.38	3.08	1.42	3.23	3.2	3.15	2.615
MnO	28.22	19.08	26.05	23.69	24.86	22.36	24.92	22.65	23.98
MgO	0.67	0.23	0.19	1.77	0.97	0.24	0.11	0.34	0.565
CaO	4.56	4.97	5.03	7.96	5.15	7.35	6.93	6.32	6.034
Na_2O	1.60	1.31	1.11	1.17	1.3	1.24	1.1	1.23	1.258
K_2O	-0.02	1.23	-0.03	1.14	0.98	0.88	0.44	0.85	0.684
P_2O_5	0.11	0.21	0.09	0.05	0.06	0.02	0.1	0.07	0.089
L.O. I	3.15	5.23	6.12	5.41	5.93	6.04	6.36	4.98	5.403
Total	100.1	99.99	99.98	99.75	100.01	99.92	100.19	99.78	99.97
Fe/Mn	0.07	0.12	0.09	0.13	0.06	0.14	0.13	0.14	0.11
Mn/Fe	13.37	8.12	10.97	7.69	17.51	6.92	7.78	7.19	9.944

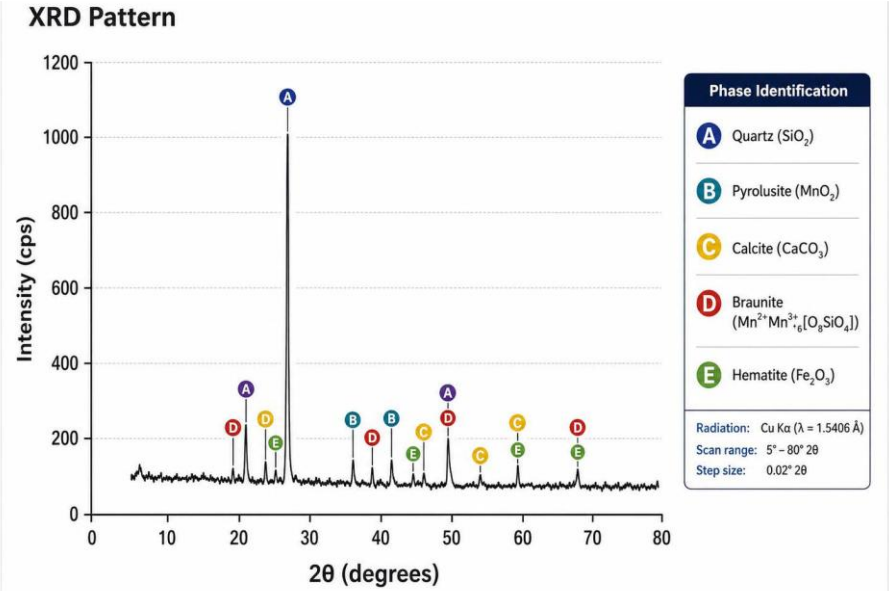

Fig. 3 XRD pattern of low-grade Mn ore showing major quartz (SiO_2) peaks with associated Mn-bearing minerals pyrolusite (MnO_2) and braunite, along with minor calcite and hematite.

well-developed euhedral to subhedral crystals, as illustrated in Figures 5C and 5D.

4.3. SIEVE AND CHEMICAL ANALYSIS

The processed sample were then crossed to sieve analysis using the ASTM standard screens, to get 1 kg representative sample. The results of the size and chemical analysis of the fractionated materials are shown in Table 2. By decreasing the size fraction, the MnO content generally decreases, while an increase in the silica content is observed. However, a lower MnO content (23.6 wt%) in the +841 µm size fraction compared to the −841 µm fraction can be attributed to the heterogeneous distribution of Mn-bearing minerals and incomplete liberation in the coarsest fraction, where Mn minerals may remain locked with silica-rich gangue. A similar trend is observed for SiO_2, reflecting the mineralogical association between Mn oxides and silicate phases.

Based on the results obtained, it is clear that Mn minerals are ground more efficiently using a disc crusher, and their distribution in coarse-size fractions (i.e. +800 to +400 µm) is greater than that in finer size fractions (<400 µm). This clarification is consistent with the enrichment trend observed in Table 2, where the highest MnO values occur in intermediate-to-coarse fractions rather than in the finest sizes. The maximum MnO content is 25.38 % in the +800 to +400 µm size fractions. From the results obtained, we can conclude that the maximum liberation of these low-grade Mn ores can be obtained in the size range mentioned above.

4.4. METHOD FOR BENEFICIATION

Pure manganese has a density of 7.26 g/cm³ (7.26 g/cc) (Lide, 2005), which is different for various manganese-bearing minerals. Braunite and pyrolusite are the principal ore minerals with specific gravities of 4.89 and 5.24 g/cc, respectively. Silica, the primary gangue mineral, is lighter and has a specific gravity of 2.65 g/cc. For gravity separation selection, the concentration criterion (CC) can be obtained from Equation 1 (Gupta and Yan, 2006; Lei et al., 2026).

$$CC = \frac{SG\ of\ heavy\ mineral - SG\ of\ fluid}{SG\ of\ lighter\ mineral - SG\ of\ fluid} \quad (1)$$

Here, CC represents the concentration criterion, which is a dimensionless parameter used to evaluate

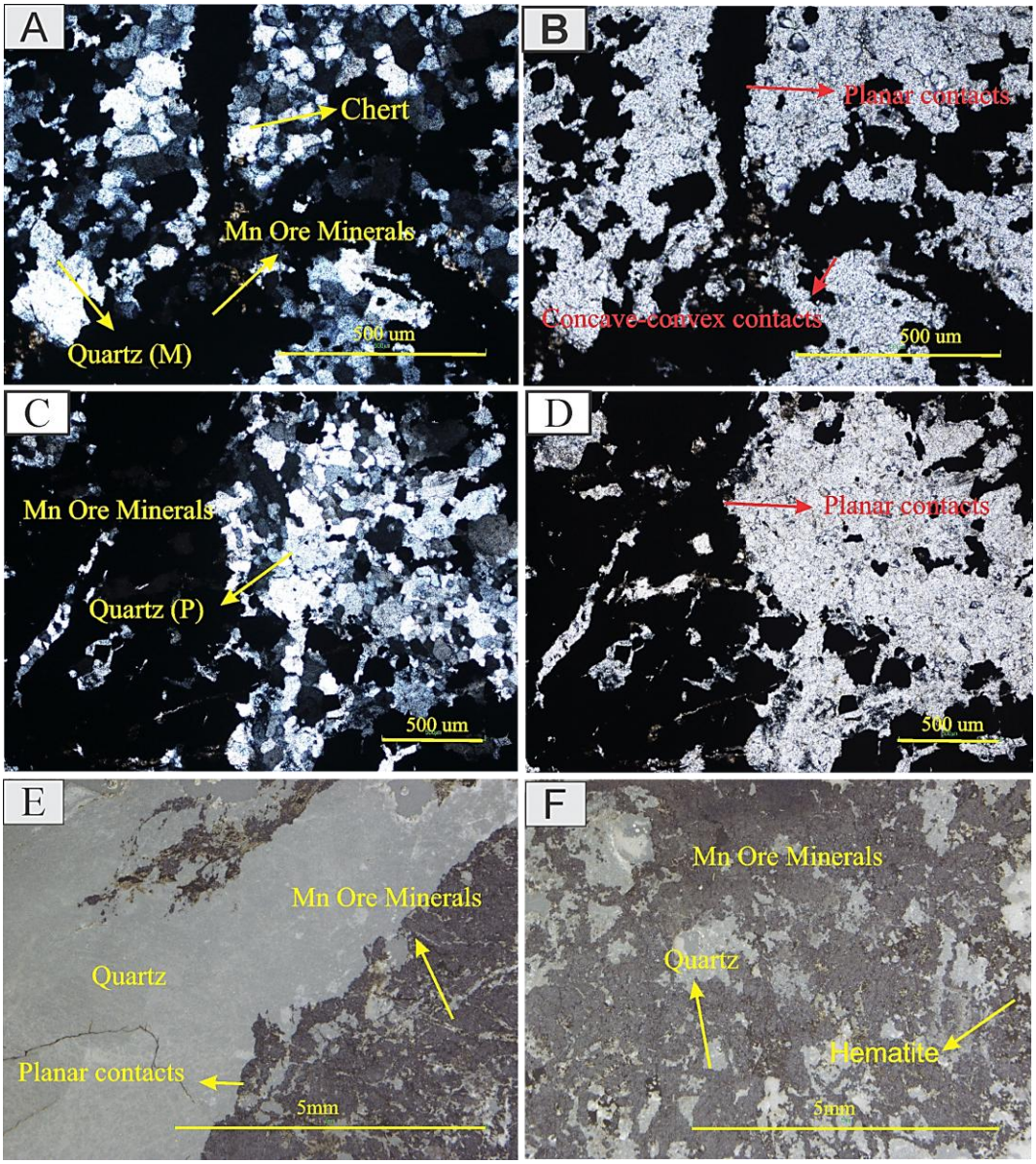

Fig. 2 Transmitted microscopy images of (A) XPL fine-grained quartz (Chert) enclosed within manganese ore minerals with interlocking contacts, (B) PL Mn ore minerals showing planar to concavo-convex contacts with gangue minerals, and (C) XPL interlocking of Mn.

the suitability of gravity separation based on density differences between valuable and gangue minerals. The specific gravity of water is taken as 1. The CC values obtained for these ores are 2.35 and 2.73 for Braunite and Pyrolusite, respectively, which are sufficient for selecting gravity separation for the understudied low-grade Mn ores.

4.5. BENEFICIATION TESTS

4.5.1. SHAKING TABLE

Shaking table tests were performed on 5 kg samples (as shown in Figure 2) with grain sizes ranging from +800 to 400 µm at deck angles of 2°, 3°, 4°, and 5°. The chemical analysis of the products obtained from shaking tables at various deck angles is shown in Table 3. The middles were subjected to the process of tabling twice to achieve maximum grade and recovery. The assays show that a prominent amount of gangue minerals and Mn minerals are also present in the concentrate product. The best results were obtained at a deck angle of 4°. The Mn grade increased from 25 % to 43.36 %, with a recovery of 67 %. The trends of MnO, SiO_2, and Fe_2O_3 at different deck angles are shown in Figure 6.

4.5.2. MAGNETIC SEPARATOR RESULTS

The concentrates obtained from the shaking table at different deck angles were tested using a magnetic separator to remove hematite and improve the Mn:Fe ratio. A low-intensity dry magnetic separator was used, primarily targeting weakly magnetic iron-bearing minerals such as hematite. Under the applied magnetic field, weakly magnetic (paramagnetic) minerals, including hematite, were attracted to the magnetic fraction, whereas nonmagnetic minerals (e.g. silica-rich gangue) reported to the nonmagnetic

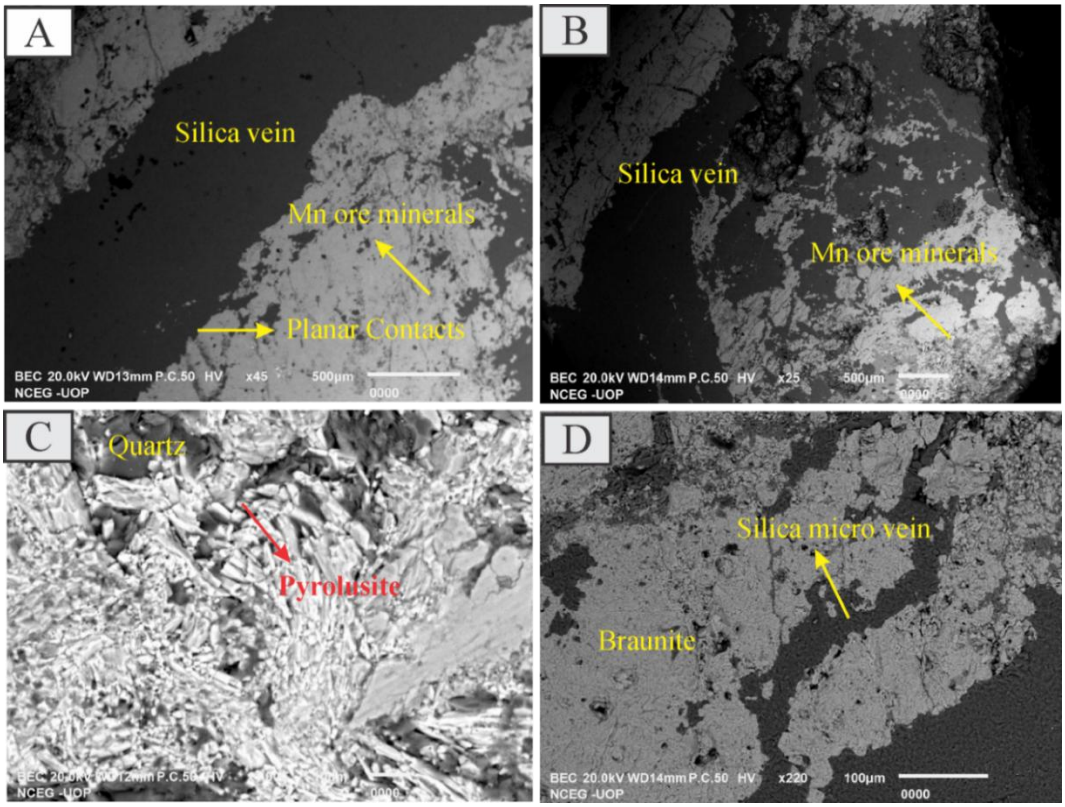

Fig. 3 (Backscattered electron images) obtained through scanning electron microscopy (A & B) Silica veinlets intruding Mn minerals showing sharps contacts. (C) Spindle-shaped pyrolusite grains enclosing microcrystalline quartz. (D) Braunite grains crosscut.

Table 2 Sieve analysis and chemical composition of each size fraction.

Total weight (1000 g)					
Mesh Size	Micron µm	Mass retained g	Mass retained %	Mn grade wt. %	Silica grade wt. %
20	+841	252	25.2	23.60	56.23
30	-841 +595	239	23.9	26.24	54.21
40	-595 +400	231	23.1	26.31	53.68
50	-400 +297	81	8.1	24.11	55.05
100	-297 +149	50	5.0	21.06	57.25
140	-149 +105	35	3.5	18.65	58.24
200	-105 +74	25	2.5	18.21	58.66
Pan	Pan	86	8.6	17.48	58.91

fraction. The maximum manganese grade reported was 45.96% MnO from the concentrate obtained by shaking the table at a deck angle of 4°. where the shaking table concentrate initially contained 43.36 % MnO. The results show that there is an increase in the Mn:Fe ratio due to the selective removal of iron-bearing minerals into the magnetic fraction, thereby enriching MnO in the nonmagnetic concentrate fraction. The Mn:Fe ratio was calculated using the weight percentages of MnO and Fe_2O_3 obtained from chemical analyses of each product (Mn:Fe= MnO wt% /Fe_2O_3 wt%). The calculated Mn:Fe ratios corresponding to Figure 6 are provided in Table 4. The maximum manganese grade was reported from the concentrate obtained by shaking the table at a deck angle of 4°, and the Mn:Fe ratio increased from 3.21 in the feed to 15.3 in the final nonmagnetic concentrate (Fig. 7).

The relationship between MnO content and the weights of concentrate and tailing products is presented in Table 4. Higher MnO grades correspond to lower concentrate weights, reflecting effective rejection of iron-rich and siliceous gangue during magnetic separation. A mass balance discrepancy was identified in Table 4, where the feed mass (378 g) does not equal the sum of concentrate (318 g) and tailing (59 g). This difference is attributed to minor material losses during handling and transfer between separation stages.

Recoveries (%) were calculated using the standard formula:

$$Recovery\ (\%) = \frac{\text{Weight of product} \times \text{MnO grade of product}}{\text{Weight of feed} \times \text{MnO grade of feed}} \times 100$$

This approach ensures consistency between grade, mass yield, and recovery values reported in Table 4.

Table 3 shows the chemical results of the products obtained through the shaking table at various deck angles.

	Assays %					Recoveries %				
Product	Wt. gm	MnO %	Fe_2O_3%	CaO %	SiO_2%	MnO %	Fe_2O_3 %	SiO_2%	CaO %	Deck angle
Feed	1000	24.05	3.98	5.85	55					
Concentrate	305	38.3	6.96	7.35	42.34	47.39	53.34	23.48	38.32	2°
Tailing	645	15.48	2.78	5.54	61.53	40.51	45.05	72.16	61.08	
Concentrate	328	40.12	6.98	6.78	40.56	53.38	57.52	24.19	38.01	3°
Tailing	638	14.21	2.56	5.65	62.44	36.78	41.04	72.43	61.62	
Concentrate	378	43.36	7.18	5.34	34.62	66.49	68.19	23.79	34.5	4°
Tailing	600	11.22	2.08	6.37	65.98	27.31	31.36	71.98	46.68	
Concentrate	356	37.25	6.68	5.64	38.65	53.8	59.75	25.02	34.32	5°
Tailing	608	16.88	2.44	6.29	63.35	41.64	37.27	70.03	65.37	

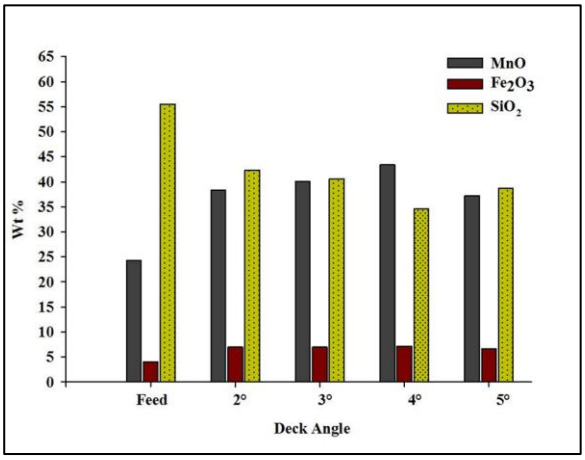

Fig. 6 Variation in MnO, Fe_2O_3, and SiO_2 contents in the concentrate obtained from the shaking table at different deck angles. The feed represents the initial ore composition, and subsequent bars show the effect of deck angles from 2° to 5° on the concentration of manganese, iron, and silica. Maximum MnO enrichment is observed at a deck angle of 4°, with concurrent reduction in silica content.

5. DISCUSSION

The low-grade Mn ores of the Mohmand district have an average MnO content of 24 %, with pyrolusite and braunite being the leading economic minerals. Mineralogical studies suggest that silica is the main gangue mineral in these ores, with 56 % on average, making them uneconomical. The silica occurs in two forms: fine-grained quartz (chert), enclosed within Mn minerals and cannot be separated at coarser grain sizes, and coarser secondary silica veins of monocrystalline quartz. The silica veins cross-cut the ore bodies, which have an average thickness greater than 1 mm, making these ores uneconomical the coarser grains of quartz show planar contact with the ore minerals, which can be easily separated. The contents of calcite and hematite are negligible, as observed in mineralogical studies. Mn-bearing minerals can be liberated at grain sizes greater than 400 µm. The densities of the two economic phases (Braunite and Pyrolusite) and major gangue minerals (Silica) differ significantly (4.89, 5.24, and 2.65 g/cm^{3,} respectively). The upgradation of these ores at a size fraction of +800 to +400 µm using gravity separation will be possible using this density contrast. The MnO content improved in the low-grade Mn ore from the district of Mohmand, as shown in Table 3. The best grade and recovery were observed at a deck angle of 4° for the feed with 25 % MnO, which increased to 43 % with a recovery of 66.7 %. Similarly, the silica content decreased to 34.62 % from an initial feed value of 56 %, indicating effective rejection of siliceous gangue at this operating condition. A decrease in the MnO content at a deck angle of 5° was observed, which can be attributed to the presence of fine-grained cherty silica enclosed within Mn-bearing minerals; this textural interlocking alters the effective density of the composite particles, causing them to report to the tailings. Hematite (Fe_2O_3), a dense and weakly magnetic iron-bearing mineral, was also concentrated in the gravity concentrate, thereby negatively affecting the Mn/Fe ratio, as confirmed by mineralogical observations and chemical analyses. Magnetic separation can therefore help upgrade these low-grade Mn ores by selectively removing iron-bearing minerals, as demonstrated by the results in Table 4. The MnO content in the concentrate obtained at a deck angle of 4° was further increased to 45.96 %, with a recovery of 89.17 %, highlighting the effectiveness of the combined gravity–magnetic separation approach.

6. CONCLUSION

The low-grade manganese ores of the Mohmand district consist of braunite and pyrolusite, which are the principal economic minerals, and silica, which is the primary gangue mineral. Economic minerals with

Table 4 show the chemical results of the products obtained through a magnetic separator.

		Assays %				Recoveries %			
Product	Wt. (g)	MnO	Fe_2O_3	CaO	SiO_2	MnO	Fe_2O_3	Fe_2O_3	SiO_2
Feed (conc. at 2 °)	305	38.3	6.96	7.35	42.34	---	---	---	---
Concentrate	265	40.76	3.41	7.44	43.74	92.47	42.57	87.94	89.76
Tailing	40	22.14	30.41	6.79	33.12	7.58	57.3	12.11	10.26
Feed (conc. at 3 °)	328	40.12	6.98	6.78	40.56	---	---	---	---
Concentrate	284	42.39	3.46	6.79	41.98	91.48	42.92	86.71	89.61
Tailing	44	25.06	29.71	6.71	31.41	8.38	57.1	13.28	10.39
Feed (conc. at 4 °)	378	43.36	7.18	5.34	34.62	---	---	---	---
Concentrate	318	45.96	3.21	5.35	36.03	89.17	37.61	84.26	87.56
Tailing	59	29.19	28.74	5.28	27.51	10.51	62.48	15.43	12.4
Feed (conc. at 5 °)	356	37.25	6.68	5.64	38.65	---	---	---	---
Concentrate	309	39.13	3.39	5.64	39.81	91.18	44.05	86.79	89.41
Tailing	47	25.13	28.31	5.49	31.05	8.91	55.95	12.85	10.61

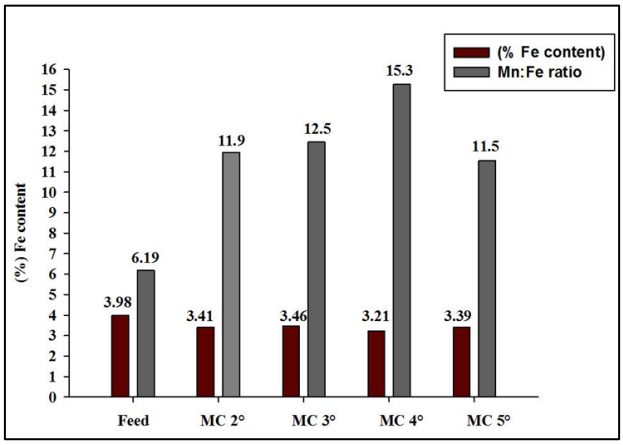

Fig. 7 Trends of the Mn:Fe ratio using a magnetic separator (MC= magnetic separator concentrates of the feed obtained through the shaking table at angles of 2°, 3°, 4°, and 5°).

different densities and magnetic properties can be easily concentrated using gravity and magnetic separation techniques. According to mineralogical data, silica and ore minerals can be liberated at coarser grain sizes. The chemical analysis of various ore fractions obtained through sieve analysis showed that the maximum Mn grade was 25 % in the size range from +800 to +400 µm. The density difference between ore minerals and silica is large enough to select gravity separation as an upgrade technique. Therefore, the ore content was increased to 43 %, nearly 67 % of which was recovered using a shaking table. Similarly, removing iron-bearing minerals through a magnetic separator increased the Mn content to 45.96 %, which could help increase the Mn/Fe ratio. These results demonstrate that low-grade Mn ores from the Mohmand district can be upgraded efficiently using combined gravity and magnetic separation techniques and can be utilized in the steel industry through small-scale on-site beneficiation plants.

ACKNOWLEDGMENT

The author extend their appreciation to Ongoing Research Funding program, (ORF-2026-327), King Saud University, Riyadh, Saudi Arabia.

AUTHOR CONTRIBUTION DECLARATION

Conceptualization, MS, and IU; methodology, IU; software, MS and SS; validation, FA, GK and RJ; formal analysis, IU and MS; investigation, IU; resources, IU; data curation, MS; writing—original draft preparation, IU and MS; writing—review and editing, LA and IA; visualization, MS; supervision, LA and IA. All authors have read and agreed to the published version of the manuscript.

CONFLICT OF INTEREST

The authors declare no conflict of Interest.

REFERENCES

Ahmad, I.: 2016, Preliminary investigations for the upgradation of North Waziristan Manganese Ore Work Design. Science, Technology and Development, 35, 1, 22–25. DOI: 10.3923/std.2016.22.25

Alshehri, F., Shahab, M., Azer, M.K., Pande, C.B. and Abanumay, F.A.: 2025, An integrated remote sensing and geochemical approach for mapping the Kamal layered mafic intrusion in the Arabian Shield, Northwest Saudi Arabia. Environ. Earth Sci., 84, 1, 1-18. DOI: 10.1007/s12665-024-11995-3

Baba, A.A., Ibrahim, L., Adekola, F.A., Bale, R.B., Ghosh, M.K., Sheik, A.R., Pradhan, S. R., Ayanda, O.S. and Folorunsho, I.O.: 2014, Hydrometallurgical processing of manganese ores: a review. JMMCE, 2, 3, 230. DOI: 10.4236/jmmce.2014.23028

Din, I.U., Shah, M.T., Liaqat, A.L.I., Asghar, A.L., Alshehri, F., Almadani, S. and Shahab, M.: 2025, Mineralogy and geochemical study of sulfide mineralization, in Kadikhel Valley, Western Kohistan Island Arc. Acta Geodyn. Geomater., 22, 2, 253–276. DOI: 10.13168/AGG.2025.0018

Ding, C., Guo, X., Xiao, C., Sui, Z. and Yang, Y.: 2025, Experimental Study on the Influence of Blast Hole Bottom Cushion Medium on Blasting Damage Characteristics and Strain Evolution of Rock Mass. Rock Mech. Rock Eng., 58, 2, 1895–1909. DOI: 10.1007/s00603-024-04276-9

Gupta, A. and Yan, D.S.: 2006, Mineral Processing and Operation. Elsevier DOI: 10.1016/B978-0-444-51636-7.X5000-1

Haider, S.K., Azimi, G., Duan, L., Anthony, E.J., Patchigolla, K., Oakey, J.E., Leion, H., Mattisson, T. and Lyngfelt, A.: 2016, Enhancing properties of iron and manganese ores as oxygen carriers for chemical looping processes by dry impregnation. Appl. Energy, 163, 41–50. DOI: 10.1016/j.apenergy.2015.10.142

Kogel, J.E., Trivedi, N.C., Barker, J.M. and Krukowski, S.T.: 2006, Industrial minerals and rocks: commodities, markets, and uses. Society for Mining, Metallurgy and Exploration

Lasheen, T., El-Hazek, M., Helal, A. and El-Nagar, W.: 2009, Recovery of manganese using molasses as a reductant in nitric acid solution. Int. J. Miner. Process., 92, 3–4, 109–114. DOI: 10.1016/j.minpro.2009.03.001

Lei, H., Bao, N., Yu, M. and Cao, Y.: 2025, Estimating and mapping tailings properties of the largest iron cluster in China for resource potential and reuse: A new perspective from interpretable CNN model and proposed spectral index based on hyperspectral satellite imagery. Int. J. Appl. Earth Obs. Geoinf., 139, 104512. DOI: 10.1016/j.jag.2025.104512

Liu, B., Zhang, Y., Lu, M., Su, Z., Li, G. and Jiang, T.: 2019, Extraction and separation of manganese and iron from ferruginous manganese ores: A review. Miner. Eng., 131, 286–303. 10.1016/j.mineng.2018.11.016

Mehdilo, A. and Irannajad, M.: 2014, Evaluation of pyrolusite flotation behavior using a cationic collector. J. Min. Sci., 50, 5, 982–993. DOI: 10.1134/S1062739114050184

Mehdilo, A., Irannajad, M. and Hojjati-Rad, M.R.: 2013, Characterization and beneficiation of Iranian low-grade manganese ore. Physicochem. Probl. Miner. Process., 49. DOI: 10.5277/ppmp130230

Naseem, S., Sheikh, S.A. and Mallick, K.A.: 1997, Lithiophorite and associated manganese mineralization in Lasbela, Balochistan, Pakistan. Geosci. J., 1, 1, 10–15. DOI: 10.1007/BF02910445

Öksüz, N. and Okuyucu, N.: 2014, Mineralogy, geochemistry, and origin of Buyukmahal manganese mineralization in the Artova ophiolitic complex, Yozgat, Turkey. J. Chem., 3. DOI: 10.1155/2014/837972

Peng, N., Pan, Q., Liu, H., Yang, Z.; and Wang, G.: 2018, Recovery of iron and manganese from iron-bearing manganese residues by multistep roasting and magnetic separation. Miner. Eng., 126, 177–183. DOI: 10.1016/j.mineng.2018.07.002

Polgári, M., Hein, J., Vigh, T., Szabó-Drubina, M., Fórizs, I., Bíró, L., Müller, A. and Tóth, A.: 2012, Microbial processes and the origin of the Úrkút manganese deposit, Hungary. Ore Geol. Rev., 47, 87–109. DOI: 10.1016/j.oregeorev.2011.10.001

Rao, H., Luo, J. and He, M.: 2026. Spatio-temporal distribution patterns, genesis, metallogenic regularity, and prospects of global potash resources. Ore Geol. Rev., 188, 107100. DOI: 10.1016/j.oregeorev.2025.107100

Rehman, W.U., Rehman, A.U., Khan, F., Muhammad, A. and Younas, M.: 2020, Studies on manganese ore beneficiation through high-intensity magnetic separator. Adv. Sci. Eng., 12, 1, 21–27. DOI: 10.32732/ase.2020.12.1.21

Shah, M. and Khan, A.: 1999, Geochemistry and origin of Mn-deposits in the Waziristan ophiolite complex, north Waziristan, Pakistan. Miner. Depos., 34, 7, 697–704. DOI: 10.1007/s001260050228

Shah, M.T. and Moon, C.J.: 2004, Mineralogy, geochemistry and genesis of the ferromanganese ores from Hazara area, NW Himalayas, northern Pakistan. J. Asian Earth Sci., 23, 1, 1–15. DOI: 10.1016/S1367-9120(03)00099-3

Shahab, M., Ali, L. and Alshehri, F.: 2025, An integrated remote sensing, petrographic, and mineralogical techniques for mapping of marble deposits in the vicinity of the ophiolite sequence in North Pakistan. Geol. Acta, 23. DOI: 10.1344/GeologicaActa2025.23.4

Siddiqui, F., Burhanuddin, K., Shaif, M. and Alam, S.: 2015, Manganese ore minerals assemblages and mineral paragenesis with the help of ore petrography and XRD studies of Balaghat District, (MP) India. Global J. Sci. Front. Res. H: Env. Earth Sci., 15, 3, 21–34.

Singh, V., Chakraborty, T. and Tripathy, S.K.: 2020, A review of low-grade manganese ore upgradation processes. Miner. Process. Extr. Metall. Rev., 41, 6, 417–438. DOI: 10.1080/08827508.2019.1634567

Sudharsan, S., Hemalatha, R. and Radha, S.: 2024, Exploring clay and silicate-based mineral profiles along Pichavaram coastal region, Tamil Nadu, with Aviris-NG hyperspectral data. J. Seism. Explor., 33, 4. DOI: 10.36922/JSE10

Sun, S., Pan, S. et al.: 2025, Prediction Model for Rock-Breaking Force and Wear of Large-Diameter Shield Disc Cutters in Hard Rock Stratum. Int. J. Numer. Anal. Meth. Geomech., 49, 17, 4076-4090. DOI: 10.1002/nag.70059

Ullah, F.: 2025, Petrographic study of Diorite and Fe-Mg Diorite from the Samar Bagh Complex: Insights from petrographic and geochemical analyses. Acta Geodyn. Geomater., 22, 1, 87–104. DOI: 10.13168/AGG.2025.0007

Zhang, S., Nechaev, V.P. et al.: 2026, Mineralogy and geochemistry of the late Permian super-high-organic-sulfur coal from the Naliang mine, Xian'an coalfield in Guangxi province, China, with emphasis on the enrichment of the critical elemental assemblage of V-Se-Mo-U. Int. J. Coal Sci. Technol., 13, 1, 12. DOI: 10.1007/s40789-025-00862-6

Zhang, W. and Cheng, C.Y.: 2007, Manganese metallurgy review. Part I: Leaching of ores/secondary materials and recovery of electrolytic/chemical manganese dioxide. Hydrometallurgy, 89, 3–4, 137–159. DOI: 10.1016/j.hydromet.2007.08.010